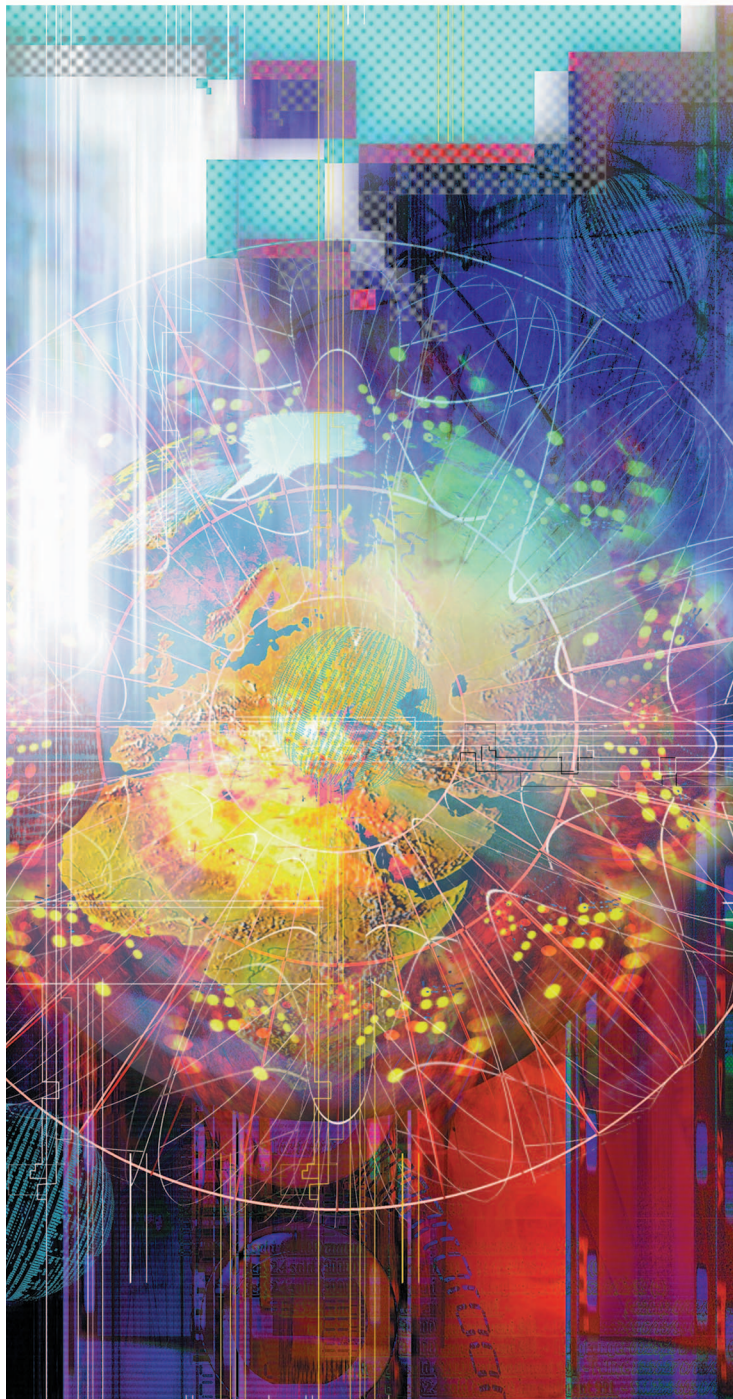


Space Mapping

Slawomir Koziel, Qingsha S. Cheng, and John W. Bandler



©DIGITAL VISION

In this article we review state-of-the-art concepts of space mapping and place them contextually into the history of design optimization and modeling of microwave circuits. We formulate a generic space-mapping optimization algorithm, explain it step-by-step using a simple microstrip filter example, and then demonstrate its robustness through the fast design of an interdigital filter. Selected topics of space mapping are discussed, including implicit space mapping, gradient-based space mapping, the optimal choice of surrogate model, and tuning space mapping. We consider the application of space mapping to the modeling of microwave structures. We also discuss a software package for automated space-mapping optimization that involves both electromagnetic (EM) and circuit simulators.

A Brief History of Microwave CAD

Early Developments

In 1967, in a benchmark paper [1], Temes and Calahan presented an extensive and detailed review of general-purpose optimization algorithms useful for computer-aided network design. They provided state-of-the-art examples of network optimization through specialized iterative techniques. Their paper was the first comprehensive review of its kind. In ensuing years, Bandler [2], [3] systematically treated the formulation of error functions with regard to design specifications. He explored least p th and minimax objectives, nonlinear constraints, gradient and direct search methods, as well as adjoint

Slawomir Koziel is with the School of Science and Engineering, Reykjavik University, Kringlunni 1, IS-103 Reykjavik, Iceland.

Qingsha S. Cheng and John W. Bandler are with the Simulation Optimization Systems Research Laboratory, Department of Electrical and Computer Engineering, McMaster University, Hamilton, ON, Canada L8S 4K1.

John W. Bandler is also with Bandler Corporation, Dundas, ON L9H 5E7, Canada.

Digital Object Identifier 10.1109/MMM.2008.929554

circuit sensitivity analysis techniques suitable for microwave circuit simulation and design.

The complexity of microwave devices has continued to increase, especially after the emergence and production of monolithic microwave integrated circuits (MMICs) [4] in the 1970s. Bandler et al. [5] demonstrated the automated optimization of a large-scale design of a 12-GHz multiplexer with 16 channels and 240 nonlinear design variables. In a 1988 review paper, Bandler and Chen [6] emphasized optimization-oriented approaches to deal more explicitly with process imprecision, manufacturing tolerances, model uncertainties, measurement errors, and so on, approaches well suited to yield enhancement and cost reduction for integrated circuits. Bandler and Salama [7] addressed circuit tuning for postproduction alignment.

Credit for the first commercial microwave circuit optimization software should be given to Les Besser for his COMPACT (Computer Optimization of Microwave Passive and Active Circuits) in 1973. Its successor, SuperCOMPACT, became an industry standard [8]. EEsof (now Agilent Technologies) launched its circuit simulator TOUCHSTONE in 1983. In 1985, Bandler introduced powerful minimax optimizers into EEsof's TOUCHSTONE. TOUCHSTONE evolved into Libra after harmonic balance simulation was added [8].

Techniques for design centering, tolerance assignment, worst-case and statistical design, and postproduction tuning evolved during the 1970s [9], peaking in the late 1980s when Optimization Systems Associates (OSA) introduced yield-driven design into SuperCOMPACT. EEsof followed suit with yield-driven design options. The 1980s also saw advances and robust implementation in software of gradient-based algorithms for minimax, l_1 , and l_2 optimization [6].

Meanwhile, during the 1980s, Ansoft Corporation, Hewlett-Packard, and Sonnet Software embarked on the development of simulators that solved Maxwell's equations for complex geometries. Denoted EM solvers or solvers, they were originally applied to obtain accurate simulations or validations of complex microwave structures.

EM-Based Optimization

The idea of employing EM solvers for direct optimal design attracted microwave engineers. However, EM solvers are notoriously CPU-intensive. As originally construed, they also suffered from nondifferentiable response evaluation and nonparameterized design variables that were discrete in the parameter space. Such characteristics are unfriendly to available efficient gradient optimization algorithms. To alleviate this, Bandler et al. proposed some breakthrough techniques, such as the utilization of databases [10]–[12], the Datapipe concept [10], multidimensional interpolation [11]–[13], geometry capture [11], [12], [14] for parameterization, and the pragmatic idea of the simulation grid. Formal EM optimization of planar and three-dimensional (3-D) microwave structures has been reported since 1994 [15]–[18].

In 1990, through Optimization Systems Associates, Bandler introduced OSA90, the world's first friendly microwave optimization engine for performance-driven and yield-driven design. It incorporated state-of-the-art microwave circuit simulation and optimization algorithms. It provided an interface to external simulators, circuit based or EM based. In Swanson's words, "[OSA90 is] the first commercially successful optimization scheme which included a field-solver inside the optimization loop" [19], [20]. The success of OSA's technology and software prompted HP (now Agilent Technologies) to acquire OSA [21].

The Space-Mapping Optimization Algorithm

Our goal is to find a fine model optimal solution

$$\mathbf{x}^* = \arg \min_{\mathbf{x}} U(\mathbf{R}_f(\mathbf{x})). \quad (1)$$

Here, the fine-model response vector is denoted by \mathbf{R}_f , e.g., $|\mathbf{S}_{21}|$ at selected frequency points. The fine-model design parameters are denoted \mathbf{x} . U is a suitable objective function. In microwave engineering, U is typically a minimax objective function with upper and lower specifications [2], [3], [6]; \mathbf{x}^* is the optimal design to be determined.

Generic space mapping uses the following iterative procedure to solve (1):

$$\mathbf{x}^{k+1} = \arg \min_{\mathbf{x}} U(\mathbf{R}_s(\mathbf{x}, \mathbf{p}^k)) \quad (2)$$

where $\mathbf{R}_s(\mathbf{x}, \mathbf{p})$ is a response vector of the space-mapping surrogate model with \mathbf{x} and \mathbf{p} as the design

variables and model parameters, respectively. In implicit space mapping [31], the model parameters are the so-called preassigned parameters. Parameters \mathbf{p}^k are obtained at iteration k using the parameter extraction procedure

$$\mathbf{p}^k = \arg \min_{\mathbf{p}} \sum_{j=0}^k w_j \|\mathbf{R}_f(\mathbf{x}^k) - \mathbf{R}_s(\mathbf{x}^k, \mathbf{p})\| \quad (3)$$

in which we try to match the surrogate to the fine model. w_j are weighting factors that determine the contribution of previous iteration points to the parameter extraction process [39]. The surrogate model is normally the coarse model \mathbf{R}_c composed with suitable transformations; e.g., the input space-mapping surrogate is defined as a linear distortion of the coarse model domain:

$$\mathbf{R}_s(\mathbf{x}, \mathbf{p}) = \mathbf{R}_s(\mathbf{x}, \mathbf{B}, \mathbf{c}) = \mathbf{R}_c(\mathbf{B} \cdot \mathbf{x} + \mathbf{c}).$$

Nevertheless, the successful interconnection of EM solvers with powerful optimization techniques only partially solved the EM-based design bottleneck, since EM simulation remained CPU-intensive. Thus, conventional mathematical optimization algorithms insufficiently satisfied the microwave community's ambitions for automated EM-based design optimization. In the 1990s, EM modeling and optimization were explored through novel technologies such as response surface modeling [13], model-reduction techniques [22], and artificial neural networks [23].

Space Mapping

In 1994, Bandler et al. [24] proposed a simple but effective idea to automatically mate the efficiency of circuit optimization with the accuracy of EM solvers. The idea was to map designs from optimized circuit models to corresponding EM models. Clearly, discrepancies were expected. A "parameter extraction" step calibrated the circuit solver against the EM simulator so that observed differences between the EM and circuit simulations were minimized. The circuit model (surrogate) was then updated with extracted parameters and made ready for subsequent efficient optimization.

This methodology is named space mapping. It utilizes a "coarse" model (analytical approximation of the physics of the device under investigation) to obtain a near optimal design of an accurate EM-based "fine" model. The coarse model may be a circuit simulator such as Agilent ADS [25]. The fine model is normally an EM simulator based on the method of moments (MoM) (e.g., Agilent Momentum [26] and Sonnet *em* [27]), finite element (e.g., Ansoft HFSS [28]), FDTD (e.g., FEKO [29]), or TLM (e.g., MEFiSto [30]). See Figure 1. A link or mapping between the fine and the coarse models is established and updated through a parameter extraction process. The mapped coarse model or updated surrogate may be re-optimized to obtain a new design.

Space-mapping optimization belongs to the class of surrogate-based optimization methods [32], which generate a sequence of approximations to the objective function and manage the use of these approximations as surrogates for optimization. In microwave and RF engineering, surrogates that can be efficiently optimized include lumped or distributed element equivalent circuit models (companion model [33]), EM scattering matrix models with tuning ports [34], [35], circuit models with embedded EM components [36], or interpolated coarse-grid EM models [37].

Surrogate-based optimization has become an EM optimization approach of choice: in [38] Rautio said, "Today, I find that most designers use either a tuning methodology, a companion modeling methodology, or some combination of the two to tune the final design with EM analysis."

In this Article

We organize our article as follows. In the next section, we recall the concept of space mapping and formulate the space-mapping optimization algorithm. We also explain and illustrate the space-mapping optimization process using a simple bandstop microstrip filter example. Then, we demonstrate the robustness of this technology through an accurate design of an interdigital filter. The subsequent sections contain an exposition of selected topics and recent developments in space-mapping technology, including implicit and output space mapping, gradient-based space mapping, as well as tuning space mapping. We also discuss the issue of an optimal choice of surrogate model to be used in space-mapping optimization, the implementation of space mapping in device modeling, as well as the Space Mapping Framework (SMF)—a user-friendly space-mapping software system.

Space Mapping Optimization

Space-Mapping Optimization Concept

The formulation of the space mapping optimization algorithm [39] is presented in "The Space-Mapping Optimization Algorithm" [31], [39]. Our goal is to obtain the fine model optimal design without direct optimization of the fine model. Instead, we want to use the surrogate model; i.e., the coarse model composed with suitable auxiliary mappings. The values of the relevant parameters of these mappings are updated during each iteration of the algorithm using a so-called parameter extraction procedure in order to obtain as good a match between the surrogate model and the fine model as possible. The surrogate model is

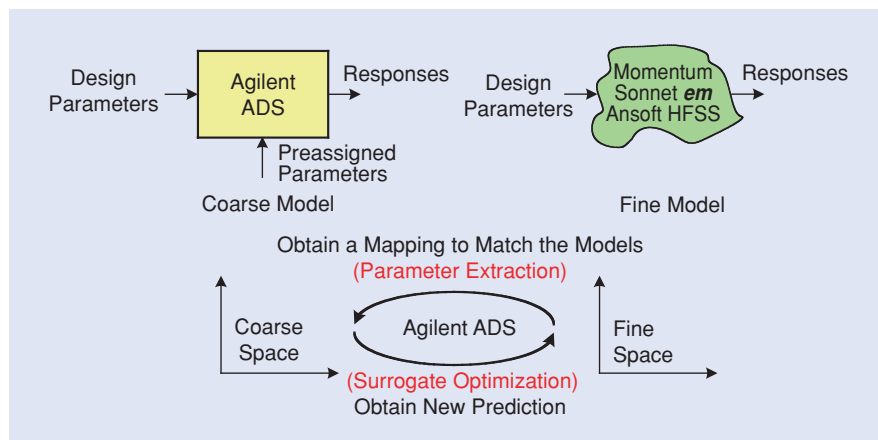


Figure 1. Space-mapping implementation concept [31].

then optimized and its optimal solution is considered to be a new design. Parameter extraction and design updating are performed solely on the surrogate model so that both require little computational overhead since the coarse model is assumed to be substantially cheaper than the fine model. The fine model is only evaluated at the new design for verification purposes and also to provide data for the next iteration of the algorithm. Typically, fine model sensitivity is not involved in the process.

A crucial prerequisite is that the coarse model is physically based; i.e., it describes the same physical phenomena as the fine model, however, with less accuracy. Due to this, the space-mapping surrogate has excellent generalization properties even if it is established using a small amount of fine model data, and the space-mapping optimization process yields satisfactory results after only few evaluations of the fine model.

Bandstop Filter Illustration

In order to illustrate the space-mapping concept let us consider a simple bandstop microstrip filter shown in Figure 2(a). We have one design parameter, the stub length L . The goal is to find L so that the center frequency of the filter is 5 GHz. The fine model is simulated in FEKO [29]. According to the space-mapping approach, instead of performing direct optimization of the fine model, we want to employ a fast surrogate model instead. The surrogate is based on the coarse model shown in Figure 2(b), which is a circuit equivalent of the structure in Figure 2(a) and is implemented in Agilent ADS [25] with the simplest form of input space mapping [39]. In particular, the surrogate is the coarse model with the design parameter L being replaced by $L + \Delta L$, where ΔL is a shift that is introduced and adjusted at each iteration to align the fine and surrogate model responses for a given L .

The process of space-mapping optimization of our filter is explained in Figure 3. We start from the optimal solution of the coarse model ($\Delta L = 0$), which is 5.6329

mm. We can observe [Figure 3(a)] that there is misalignment between the coarse and fine model responses. Also, the center frequency of the filter is 4.896 GHz instead of the required 5.000 GHz. One should note that even the initial guess is not bad, because it was obtained as an optimal solution of a physically based coarse model. The shift ΔL is adjusted to 0.120 mm in the parameter extraction process [Figure 3(b)] so that the misalignment between the fine and surrogate models is reduced. Note that a very good overall match is actually obtained, which is, again, because of the fact that the coarse model is physically based. The next step is the surrogate model optimization [Figure 3(c)], in which the length of the surrogate model stub is optimized to obtain the center frequency of 5 GHz. The new $L = 5.5129$ mm is now applied to the fine model. The corresponding center frequency of the filter is 4.999 GHz. Thus, an almost perfect design has been obtained in a single iteration of the space mapping algorithm; i.e., two evaluations of the fine model.

The design can be further improved by applying the second iteration of the algorithm, which is illustrated in Figure 3(d) and (e). The final design is $L = 5.5119$ mm, and the corresponding center frequency is exactly 5 GHz as required.

For comparison purposes, we also performed direct optimization of our filter using Matlab's *fminimax* routine [40]. Direct optimization of the fine model requires 63 fine model evaluations and yields the same design as the one obtained with the space-mapping algorithm. Thus, space mapping allows us to optimize a design substantially faster than the classical, gradient-based method. The principal reason is that the space mapping exploits knowledge embedded in a physically based coarse model. This knowledge allows us to obtain good global or quasi-global matching between the fine model and the surrogate with a small amount of fine model data and approach the optimal fine model design quickly, typically after a few iterations of the space-mapping algorithm.

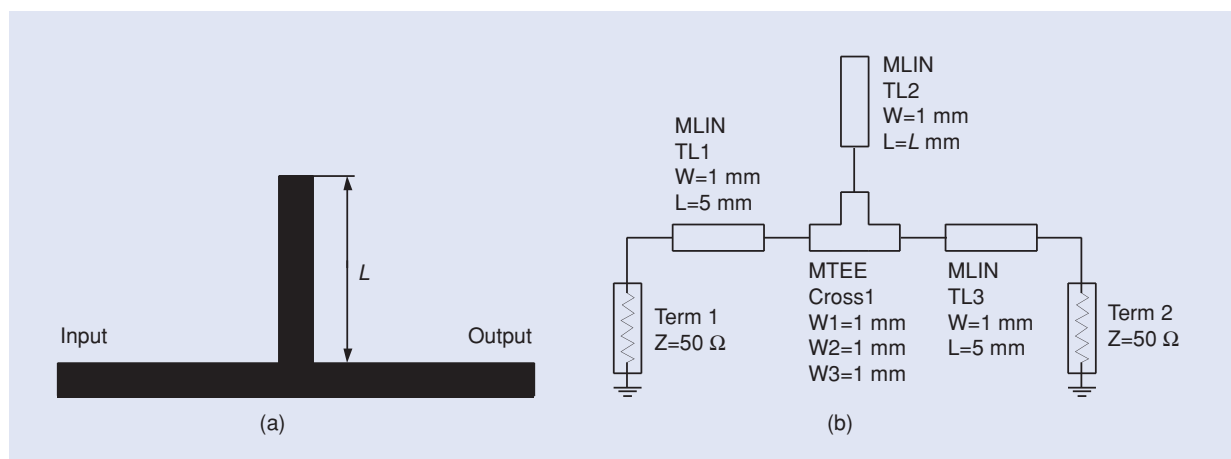


Figure 2. Simple bandstop microstrip filter: (a) geometry and (b) coarse model (Agilent ADS).

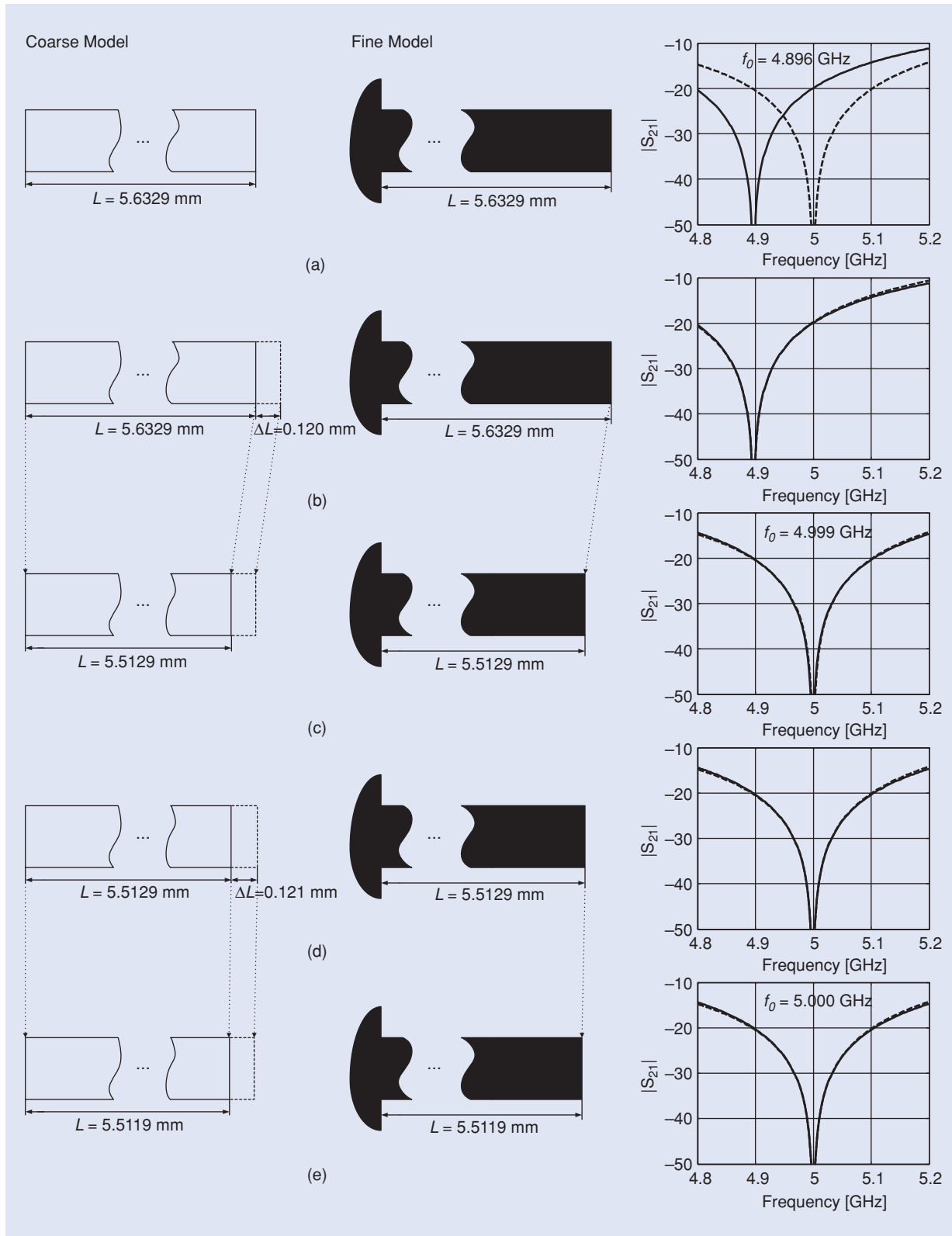


Figure 3. Space-mapping optimization of the bandstop filter; white and black rectangles represent the coarse and the fine model stub, respectively. Fine and coarse model responses on the plots are represented by solid and dashed lines, respectively: (a) initial design $L = 5.6329$ mm (coarse model optimal design), center frequency of the filter is $f_0 = 4.896$ GHz; (b) parameter extraction: ΔL is adjusted to 0.120 mm in order to align the coarse model response with the fine model response; (c) surrogate model optimization: L of the coarse model is optimized so that the center frequency of the model at $L + \Delta L$ is 5 GHz; the new L is 5.5129 mm and the filter center frequency is now 4.999 GHz; (d) second iteration (parameter extraction): ΔL is re-adjusted to 0.121 mm; (e) second iteration (surrogate optimization): the final L is 5.5119 mm and the center frequency of the filter is 5.000 GHz, as required.

Design of Interdigital Filter

In order to demonstrate the efficiency and robustness of space mapping we consider an interdigital filter design [41]. The fine model, shown in Figure 4, is implemented in Sonnet *em* [27]. The substrate height and the dielectric constant are 15 mil and 9.8, respectively. The shielding cover height is 75 mil. The cell size is set at 1 mil \times 1 mil. The design specifications are $|S_{21}| \leq -30$ dB for 4.0 GHz $\leq \omega \leq 4.5$ GHz and for 5.45 GHz $\leq \omega \leq 6.0$ GHz and $|S_{11}| \leq -0.1$ dB for 4.9 GHz $\leq \omega \leq 5.3$ GHz.

The initial Agilent ADS coarse model is shown in Figure 5. To obtain a more accurate coarse model, we insert capacitors between nonadjacent microstrip lines

as in Figure 6. For this problem, we adopt the input and implicit space mapping approaches. In the interdigital filter case, the lengths of the microstrip lines ($x_1, x_2, x_3, x_4, x_7,$ and x_8) and the gaps (x_5 and x_6) are defined as design parameters. The implicit space-mapping explores the preassigned parameters in an attempt to match the details of the surrogate to the fine model. For the interdigital filter, the preassigned parameter set consists of ϵ_r (substrate dielectric constant) and capacitors C_1 to C_6 added between nonadjacent conductors (Figure 6). The parameters for input space mapping are the shifts of design parameters; i.e., $\delta x_i, i = 1, \dots, 8$. We combine the input and implicit space mapping in one parameter extraction step.

We start our design using the optimal design from [41]. We can see that the specification is not satisfied after the first iteration, but the parameter extraction using input and implicit space mapping yields a good match between the coarse and fine model (Figure 7). The coarse model is then (re)optimized and the on-grid solutions are exhaustively searched near the optimum. In just two space-mapping iterations, a good fine model solution is obtained (Figures 8 and 9). An accurate surrogate is also obtained. The on-grid fine solution is $x_1 = 12, x_2 = 30, x_3 = 15, x_4 = 22, x_5 = 31, x_6 = 36, x_7 = 16,$ and $x_8 = 21$ (dimensions in mil).

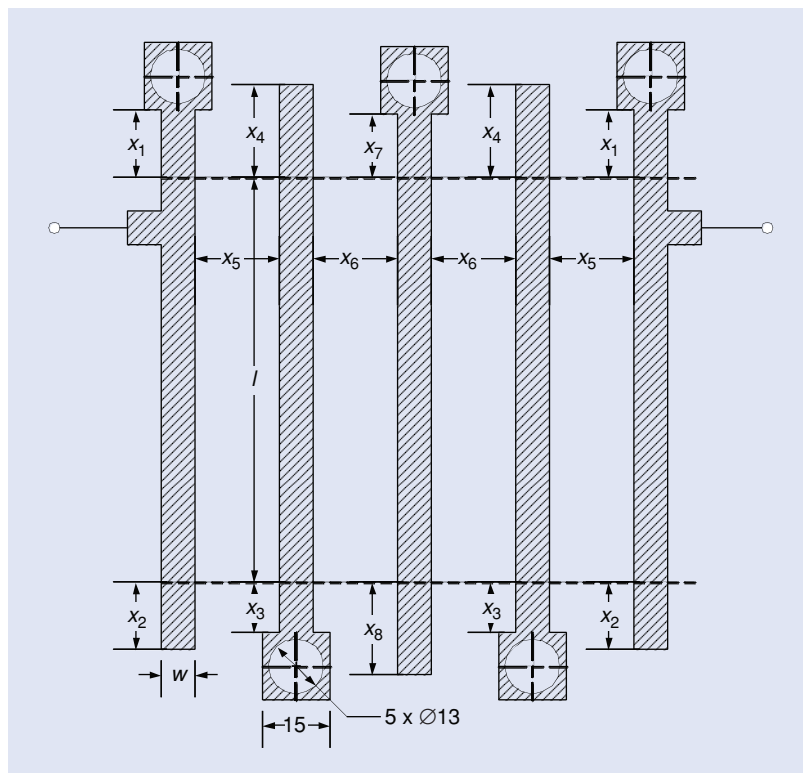


Figure 4. Interdigital filter: fine model structure and dimensions [41]; the dimensions are in mils.

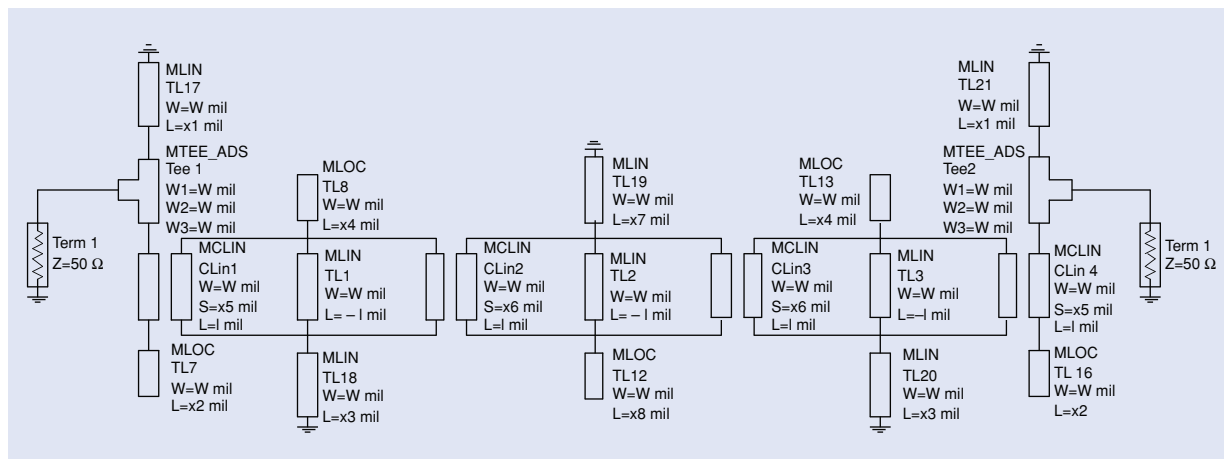


Figure 5. Initial ADS implementation of the five-conductor microstrip interdigital filter.

model are separate from the design variables, although they are still typically physically based; e.g., dielectric constant and the height of the substrate. These parameters are normally selected and their values fixed early in the modeling and design process. Implicit space mapping explores their flexibility in the design optimization [31] and device modeling [43] tasks. The effects on the responses of microwave components of varying the values of these parameters may be as significant as those achieved by varying the design parameters. Implicit space mapping (or preassigned) parameters can also be introduced to enhance the flexibility of the coarse model. Another advantage of implicit space mapping is that, unlike input space mapping [39], it does not affect the domain of the surrogate model, which may be important in the case of constrained optimization.

Consider the second-order tapped-line microstrip filter [44] shown in Figure 10(a). For the sake of simplicity we only use two design parameters, L_1 and g as defined in Figure 10(a). The fine model is simulated in

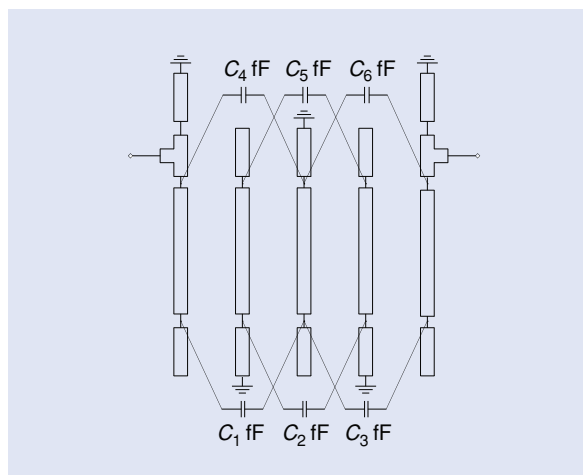


Figure 6. Interdigital filter: coarse model. Capacitors are inserted between nonadjacent transmission lines.

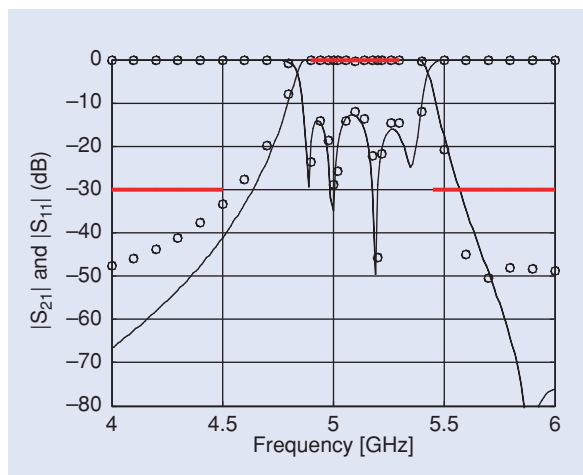


Figure 7. Interdigital filter initial design using parameters from [41]: the $|S_{11}|$ and $|S_{21}|$ responses of the fine model simulation (\circ) versus the coarse model after the first parameter extraction (—).

FEKO [29]. The design specifications are $|S_{21}| \geq -3$ dB for $4.75 \text{ GHz} \leq \omega \leq 5.25 \text{ GHz}$, and $|S_{21}| \leq -20$ dB for $3.0 \text{ GHz} \leq \omega \leq 4.0 \text{ GHz}$ and $6.0 \text{ GHz} \leq \omega \leq 7.0 \text{ GHz}$. The coarse model shown in Figure 10(b) is the circuit equivalent of the structure in Figure 10(a), and is implemented in Agilent ADS [25].

We want to optimize our filter using implicit space mapping with the dielectric constant ϵ_r and height H of the substrate as preassigned parameters. Initial values of the parameters are 9.9 and 100 mil, respectively, for both fine and coarse models. These parameters remain fixed in the fine model; however, we are going to tune them in the coarse model, according to the implicit space-mapping methodology.

The initial design, $L_1 = 6.977 \text{ mm}$ and $g = 0.060 \text{ mm}$, is the optimal solution of the coarse model with respect to our specifications. Figure 11(a) shows the fine and coarse model responses at the initial design. Note that neither the coarse nor fine models satisfy the design specifications. Also, there is quite a significant

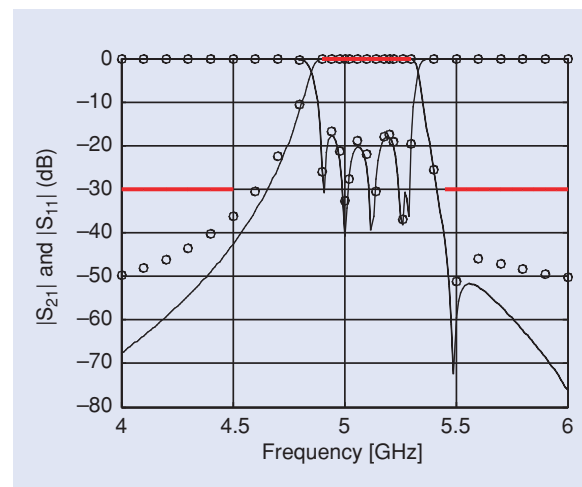


Figure 8. The interdigital filter $|S_{11}|$ and $|S_{21}|$ responses of the fine model final simulation (\circ) versus the surrogate model (—).

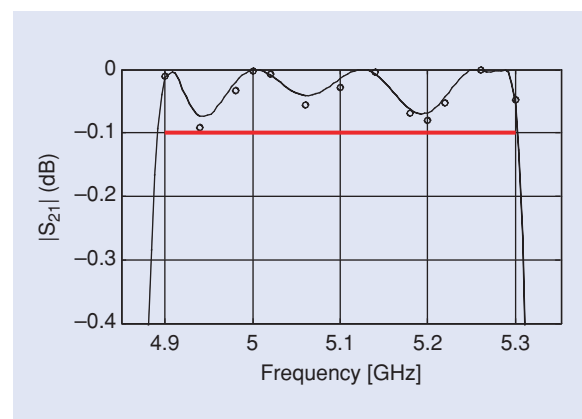


Figure 9. The interdigital filter $|S_{11}|$ and $|S_{21}|$ passband details of the fine model final simulation (\circ) versus the surrogate model simulation (—).

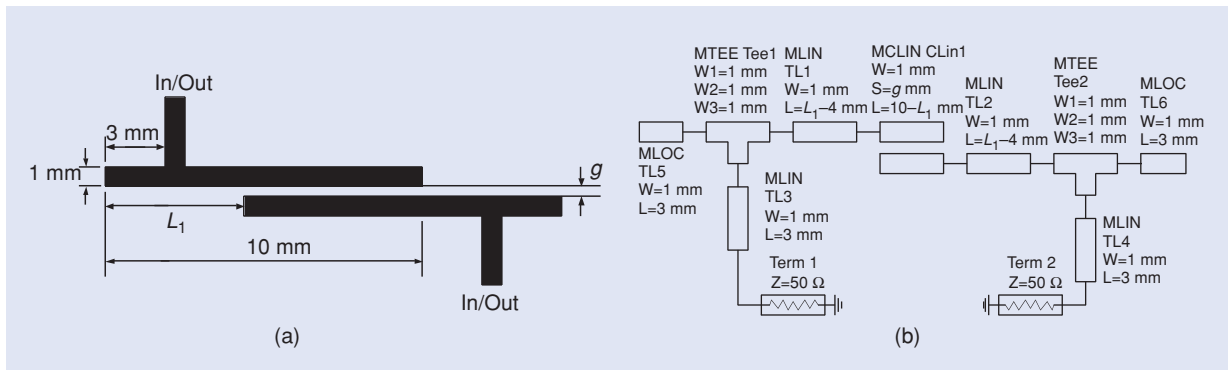


Figure 10. Second-order tapped-line microstrip filter [44]: (a) geometry and (b) coarse model (Agilent ADS).

misalignment between the fine and coarse models both with respect to center frequency and bandwidth. We now perform the parameter extraction procedure and update ϵ_r and H so that the misalignment between the

fine and the coarse model is minimized. The new values are $\epsilon_r = 10.37$ and $H = 78.1$ mil. Figure 11(b) shows the fine model and the updated coarse model response at the initial design. We (re)optimize the design parameters in our coarse model with the newly obtained preassigned parameter values. A new set of design parameter values, $L_1 = 6.419$ mm and $g = 0.053$ mm, is found and supplied to the fine model. Fine and coarse model responses at this new design are shown in Figure 11(c). We can observe that the fine model response satisfies the design specifications.

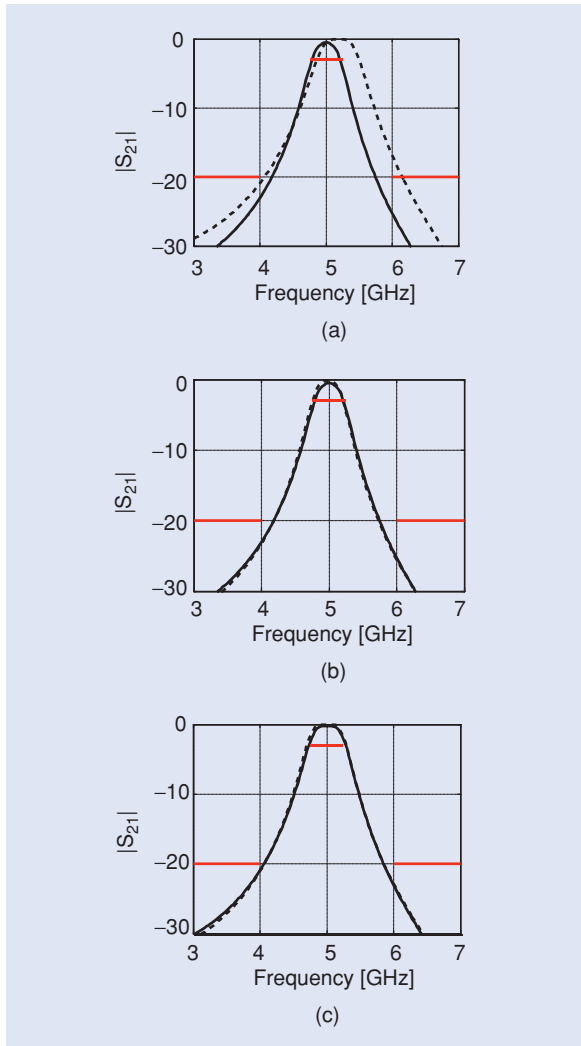


Figure 11. Second-order tapped-line microstrip filter: fine model (—) and coarse model (- -) responses. (a) the initial design, (b) a good match obtained after extracting the pre-assigned parameters, and (c) a good fine model response at the optimal design of the updated coarse model.

Output Space Mapping, Gradient-Based Space Mapping, and Trust Region Methods

It is important for the performance of space mapping that the surrogate model is a sufficiently good representation of the fine model. Typically, a proper physically based coarse model and a right combination of mappings ensure good global matching between the models. However, this may not be enough to precisely locate the fine model optimum. Therefore, so-called output space mapping has been proposed [39], [45]. In its simplest form, the output space mapping enhances the (original) surrogate model by a correction term that is nothing else but the difference between the fine and the original space-mapping responses at the current iteration point so that a perfect match between these models is ensured (which is also called a zero-order consistency condition [46]).

In order to illustrate the benefits of output space mapping, consider the microstrip bandpass filter shown in Figure 12(a) [47]. The fine model is implemented in FEKO [29], the coarse model is a circuit equivalent of the structure in Figure 12(a) implemented in Agilent ADS [25] [Figure 12(b)]. Figure 13(a) shows the fine (solid line) and the (frequency) space mapping surrogate (dashed line) model responses at a certain iteration of the space-mapping algorithm, say, iteration i . Figure 13(b) shows the response of the optimized surrogate model as well as the fine model response at the surrogate model optimum. If the surrogate model is enhanced by the output space-mapping term, its response becomes identical to the fine model response at Figure 13(a). If we now

optimize this enhanced model, we end up at a different design for which the corresponding fine and surrogate model responses are shown in Figure 13(c). We can observe that the fine model response at Figure 13(c) is better than the response at Figure 13(b) with respect to the given specification (specification error +2.3 dB versus +0.4 dB). The reason is that the output space-mapping correction term compensates the misalignment between the fine and surrogate model [Figure 13(a)] and, although it only provided perfect alignment at the current design, it also reduces the mismatch between the models in the neighborhood of this design.

The surrogate model can be further enhanced by adding an additional term that is a linear function

of the design variables, and which is designed so that the Jacobian (the first-order derivatives) of the surrogate model coincides with the Jacobian of the fine model at the current design [39] (first-order consistency condition [46]). This additional term involves fine model sensitivity information, which increases the computational cost of the space-mapping optimization process; however, it makes it more robust at the same time as it ensures the convergence of the algorithm to (at least) a local fine model optimum if the algorithm is equipped with the trust region methods mechanism [48]. Theoretical aspects of the output and gradient-based space mapping are discussed in [39].

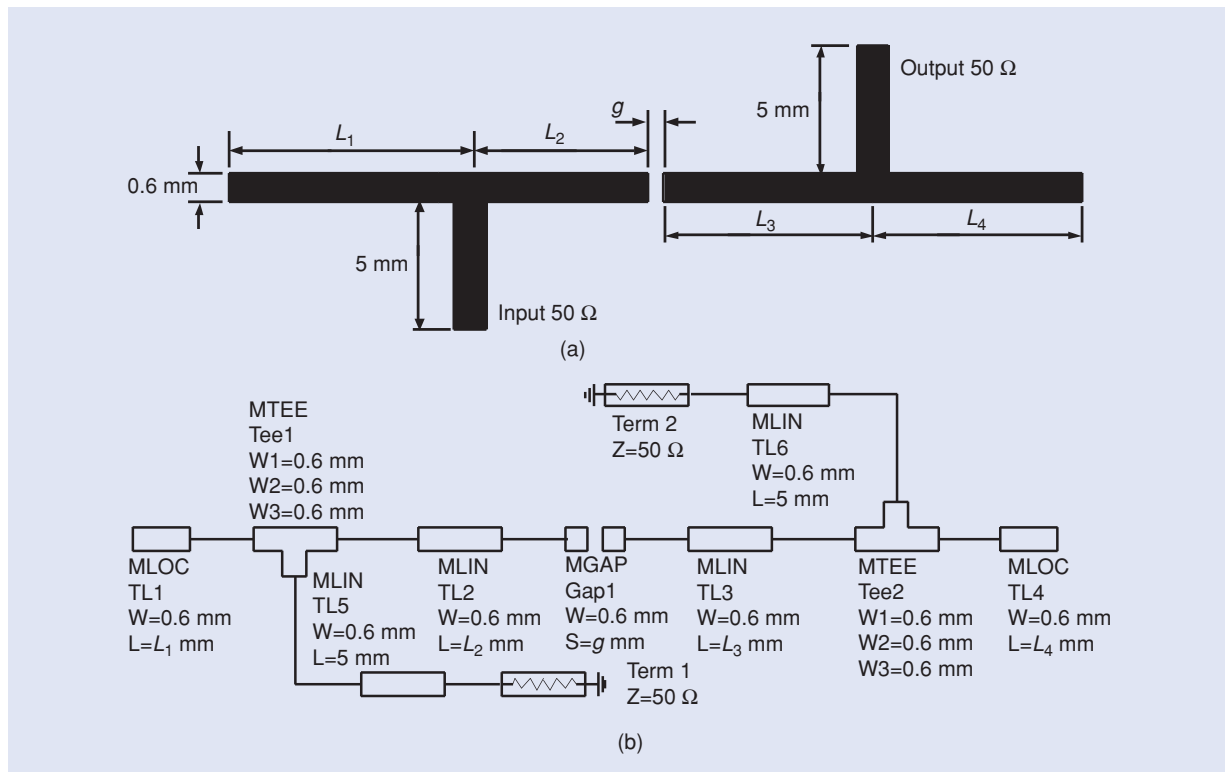


Figure 12. Microstrip bandpass filter [47]: (a) geometry and (b) coarse model (Agilent ADS).

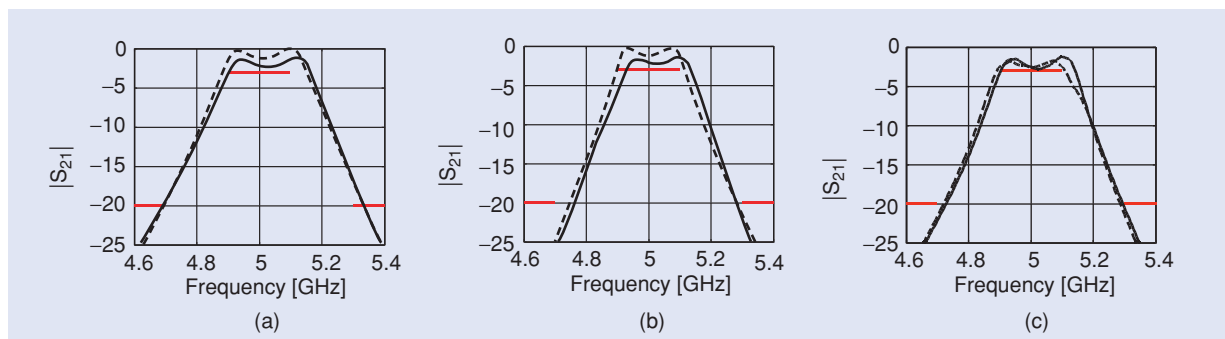


Figure 13. Output space mapping advantages (fine and surrogate model responses shown as solid and dashed lines, respectively): (a) the fine and surrogate model responses at iteration i of the space-mapping algorithm (fine model specification error +4 dB), (b) the response of the optimized surrogate and the fine model response at the surrogate model optimum (fine model specification error +2.3 dB), and (c) the response of the optimized surrogate enhanced by the output space mapping correction term and the fine model response at the enhanced surrogate model optimum (fine model specification error +0.4 dB).

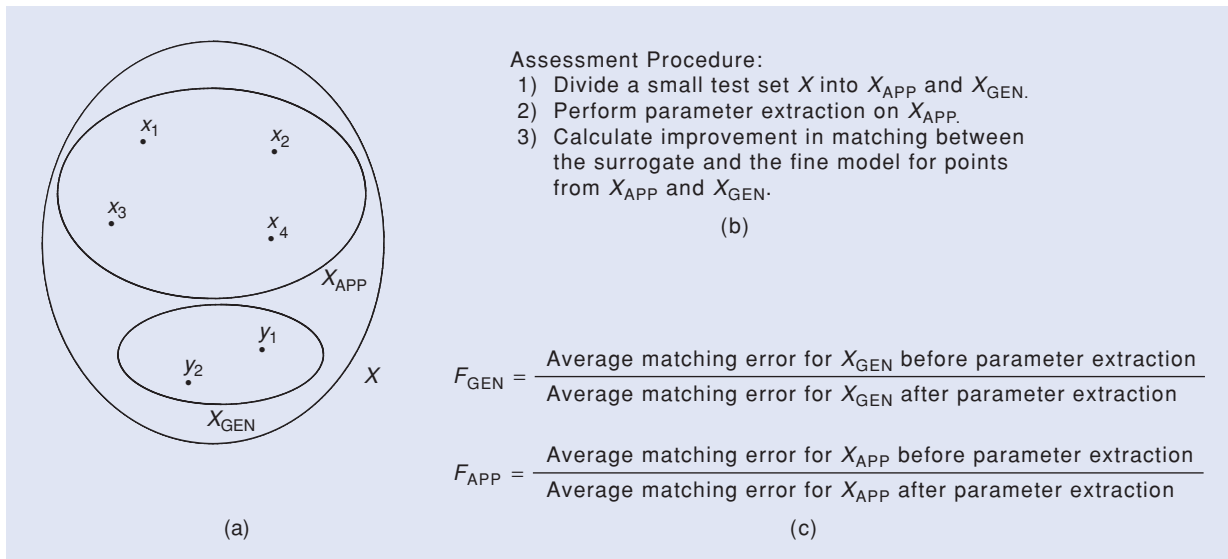


Figure 14. Space mapping assessment: (a) the test set X and the two subsets X_{APP} and X_{GEN} , (b) the assessment procedure, and (c) the quality factors.

Surrogate Model Choice and Adaptive Space Mapping

Basic space mapping types can be combined to create more involved surrogate models [39]. Having a number of mapping types available, the number of possible combinations is even larger. Given a design problem, we need to choose the most suitable coarse model and space-mapping approach and this choice is far from obvious. In general, combining different kinds of space mapping and introducing new parameters improves the flexibility of the surrogate model. On the other hand, a proper choice of the space mapping is usually problem dependent. We do not want the surrogate model to be too simple, because in that case it cannot properly reflect the features of the fine model. Also, we do not want the surrogate to be over-flexible, because its generalization properties may be then lost [49]. A suitable choice of space mapping requires both knowledge of the problem and engineering experience, although some research

has been done on automatic procedures to help in this process [49]–[51].

One such procedure is based on estimating the approximation and generalization capabilities of the surrogate model [49]. The idea is shown in Figure 14. Assume that we have a set of test points X , which we divide into two subsets, X_{APP} and X_{GEN} . We perform extraction of the surrogate model parameters on X_{APP} and then calculate the improvement of matching between the surrogate and the fine model for points from both subsets. In particular, we calculate two quality coefficients: F_{APP} , the average matching improvement of the surrogate model for points at which we performed parameter extraction, and F_{GEN} , the average matching improvement for points not used in parameter extraction. F_{APP} and F_{GEN} estimate the approximation and the generalization capability of the surrogate model, respectively. Using our factors we can now distinguish between different surrogate models and choose

the one that exhibits the highest value of F_{APP} and/or F_{GEN} .

Let us consider the seven-section impedance transformer example [50]. Here, both fine [Figure 15(a)] and coarse [Figure 15(b)] models are circuit models implemented in Matlab. The fine model consists of seven transmission lines loaded with capacitors. The coarse model consists only of transmission lines. The lengths of the lines are our design variables.

We consider four surrogate models that use input space mapping, input and implicit

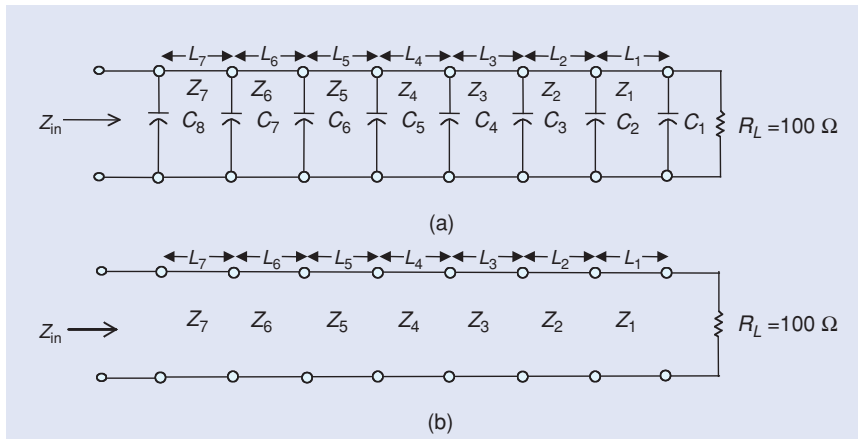


Figure 15. Seven-section capacitively loaded impedance transformer: (a) the “fine” model and (b) the “coarse” model [50].

TABLE 1. Surrogate models, quality factors and optimization results for the seven-section transformer example.

Surrogate Model					
Model No.	Formula	Description	F_{APP}	F_{GEN}	Final Specification Error*
1	$R_c(\mathbf{B} \cdot \mathbf{x} + \mathbf{c})$	(Full) input space mapping	3.7	1.4	0.00684
2	$R_c(\mathbf{B} \cdot \mathbf{x} + \mathbf{c}, \mathbf{x}_p)$	(Full) input and implicit space mapping	4.4	1.7	0.00450
3	$\mathbf{A} \cdot R_c(\mathbf{x} + \mathbf{c})$	Output and input space mapping	14.6	6.6	-0.00906
4	$\mathbf{A} \cdot R_c(\mathbf{x} + \mathbf{c}, \mathbf{x}_p)$	Output, input and implicit space mapping	27.2	11.7	-0.00939

*Specification error value after six iterations of the space-mapping optimization algorithm. The specification error at the actual fine model optimum is -0.00987.

space mapping, as well as two models using a multiplicative output space mapping. For each model, we calculate the F_{APP} and F_{GEN} factors and then perform space-mapping optimization. The values of the final specification error obtained after six iterations are shown in Table 1. As we can see both approximation and generalization capability is much better for models 3 and 4 than for models 1 and 2. This means that models 3 and 4 are more suitable for our problem than models 1 and 2. This is reflected by the values of the specification error: the space mapping algorithm working with models 1 and 2 failed to find a solution satisfying the design specifications. In contrast, the algorithm using models 3 and 4 found solutions that are very close to the actual fine model optimum.

The assessment procedure can be performed, as demonstrated above, as a stand-alone process before performing the actual optimization, or it can be embedded into the space-mapping algorithm so that a choice of the most suitable model is done before each iteration of the algorithm [49]. Other assessment methods are available that take into account other factors, such as estimated convergence properties of the algorithm using a particular surrogate model or the ability of the model to satisfy the design specifications [51].

Expert Approach: Tuning Space Mapping

Tuning space mapping [52] is a specialized version of the space-mapping approach that brings together the concepts of tuning [53], [54] and space mapping. The surrogate model's role is taken by a so-called tuning model, which could be constructed by introducing circuit-theory-based components (e.g., capacitors, inductors, or coupled-line models) into the fine model structure, and the parameters of these circuit components are chosen to be tunable. In each iteration, the tuning model is updated and optimized with respect to the tun-

ing parameters. This process takes little CPU effort as the tuning model is typically implemented within a circuit simulator. With the optimal tuning parameters thus obtained, a calibration is needed to transform these tuning values into an appropriate modification of the design variables, which are then assigned to the fine model. The calibration process involves an auxiliary model, typically a fast space-mapping surrogate, or can use analytical calibration formulas if they are known. The structure of the tuning model as well as a proper selection of tuning elements are crucial to the performance of the overall optimization process and normally require significant engineering expertise. The conceptual illustration of the tuning model is shown in Figure 16.

Microstrip Line Illustration

Consider the microstrip transmission line [53] example shown in Figure 17(a). The fine model is implemented in Sonnet *em* [27], and the fine model response is taken as the inductance of the line as a function of the line's length. Our goal is to find a length of line so that the corresponding inductance is 6.5 nH at 300 MHz. The original length of the line x is chosen to be 400 mil with the inductance of 4.38 nH.

We apply tuning space mapping. The tuning model is developed by dividing the structure in Figure 17(a) into two separate parts ($L1 = x/2$ and $L2 = x/2$) and adding

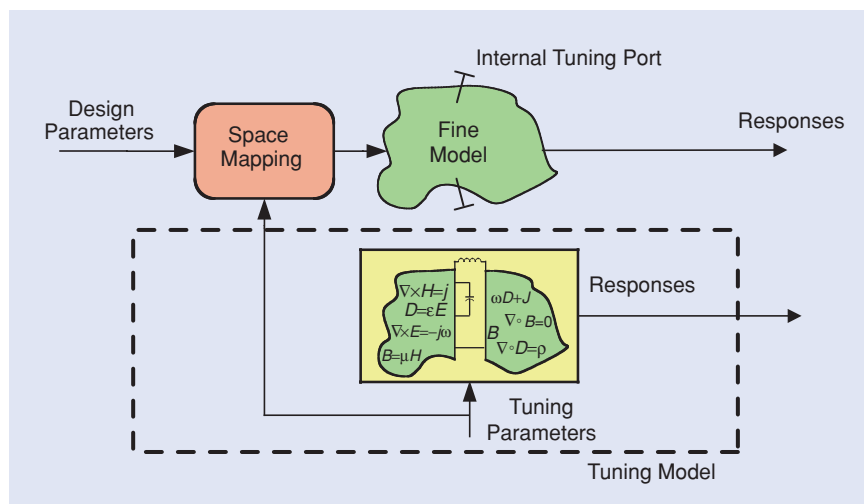


Figure 16. The concept of the tuning model for tuning space mapping [52].

the two tuning ports as shown in Figure 17(b). A small inductor is then inserted between these ports as a tuning element. The tuning model is implemented in Agilent ADS [25] and shown in Figure 18(a). The model contains the fine model data at the initial design in the form of the S4P element as well as the tuning element (inductor). Because of Sonnet's co-calibrated ports, there is perfect agreement between the fine and tuning model responses when the value of the tuning inductance L_t is 0 nH in Figure 18(a).

Next, we optimize the tuning model [Figure 18(a)] to meet our target inductance of 6.5 nH. The optimized value of the tuning inductance L_t is 2.07 nH.

Now, we need to perform the calibration step. We use the calibration model with $L_t = 0$ nH shown in Figure 18(b) in which the dielectric constant ϵ_r of the microstrip element (original value 9.8) is used as a space-mapping parameter. The value of this parameter is adjusted to 23.7 so that the response of the calibration model is 4.38 nH at $x = 400$ mil; i.e., it agrees with the fine model response at the original length of the line.

The last step is to obtain the new value of the microstrip length. We optimize the length of the line x in the calibration model [Figure 18(b)] with the tuning inductance L_t set to 0 nH to match the total inductance of the calibration model to the optimized tuning model

response, 6.5 nH. The result is $x = 586$ mil and it represents a new microstrip line design; the fine model response obtained by Sonnet *em* simulation is 6.48 nH, which is almost perfect. This result can be further improved by performing a second iteration of the tuning space-mapping algorithm, which makes the length of the microstrip line x equal 588 mil and its corresponding inductance exactly 6.5 nH.

High-Temperature Superconducting Filter Example

Tuning space mapping typically allows us to obtain acceptable results even faster than with the standard space mapping, providing that the tuning model is carefully designed. Figure 19(a) shows the structure of the high-temperature superconducting (HTS) band-pass filter [55]. The design parameters are the lengths of the coupled lines and the spacing between them. Design specifications are $|S_{21}| \geq 0.95$ for 4.008 GHz $\leq \omega \leq 4.058$ GHz, and $|S_{21}| \leq 0.05$ for $\omega \leq 3.967$ GHz and $\omega \geq 4.099$ GHz. The fine model is simulated in Sonnet *em* [27]. The tuning model is constructed by dividing the five coupled line polygons in the middle and inserting the tuning ports at the new cut edges. Its S22P data file is then loaded into Agilent ADS. The

circuit-theory coupled line components and capacitor components are chosen to be the tuning elements and are inserted into each pair of the tuning ports [Figure 19(b)].

The calibration model is implemented in ADS and shown in Figure 20. It contains the same tuning elements as the tuning model. It mimics the division of the coupled lines performed while preparing the tuning model. The calibration model also contains six (implicit) space-mapping parameters that are used to match the calibration model with the fine model.

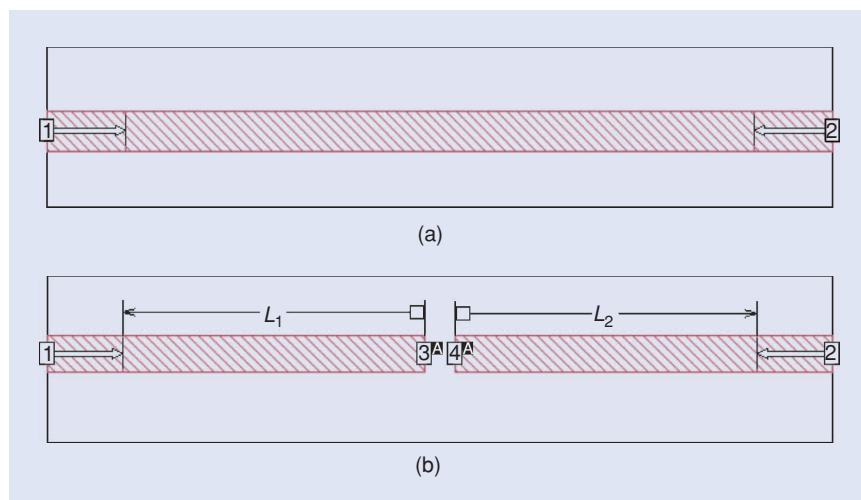


Figure 17. Microstrip line: (a) the original structure in Sonnet *em* and (b) the divided microstrip line with inserted co-calibrated ports [52], [53].

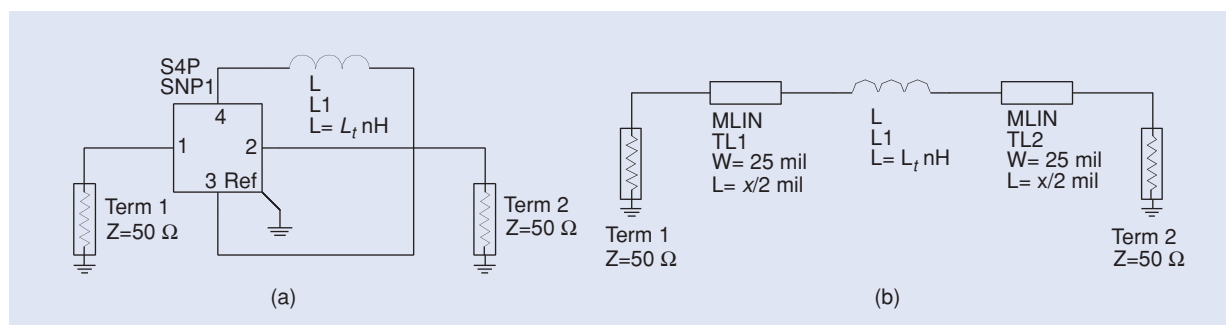


Figure 18. Microstrip line design problem: (a) the tuning model and (b) the calibration model [52], [53].

Figure 21(a) shows the fine model response at the initial solution and the response of the optimized tuning model. Figure 21(b) shows an almost equal-ripple fine model response at the final design obtained after two tuning space mapping iterations.

Space Mapping for Modeling

Although space mapping is primarily used for optimization it can also be used for modeling purposes [43], [57], [58]. The main difference is that in the case of optimization we are more focused on the local properties of the surrogate model, while for modeling we try to obtain a good global or quasi-global match between the fine and surrogate models. The most typical application of space mapping in the context of modeling is statistical analysis and yield estimation [59] of the fine model that typically requires many random samples within a given region of interest and can be made much cheaper if we use a surrogate model instead.

The space-mapping surrogate model for modeling purposes is obtained by evaluating the fine model at a number of base points located within the region of

interest; i.e., a subset of the design variable space where we want the surrogate model to be valid, then performing the usual extraction of model parameters using the gathered fine model data. It should be noted that the amount of fine model data used in space-mapping models and necessary to obtain reasonably good accuracy is surprisingly small in comparison with other methods (e.g., linear or quadratic approximation [60], radial basis functions [60], kriging [61], or neural networks [62]). This is because we assume that the underlying coarse model contains some knowledge about the physical phenomena described by the fine model, and this is what allows us to obtain a good match using just a few fine model evaluations.

Let us consider an example, which is the bandstop microstrip filter [63] shown in Figure 22(a). The fine model is implemented in Sonnet *em* [27]. We have five design variables: W_1 , W_2 , L_0 , L_1 and L_2 . It takes about one hour to evaluate the fine model for any given design. The coarse model [Figure 22(b)] is a circuit equivalent of the filter simulated in Agilent ADS and it takes just a couple of milliseconds to evaluate this model. We want to perform

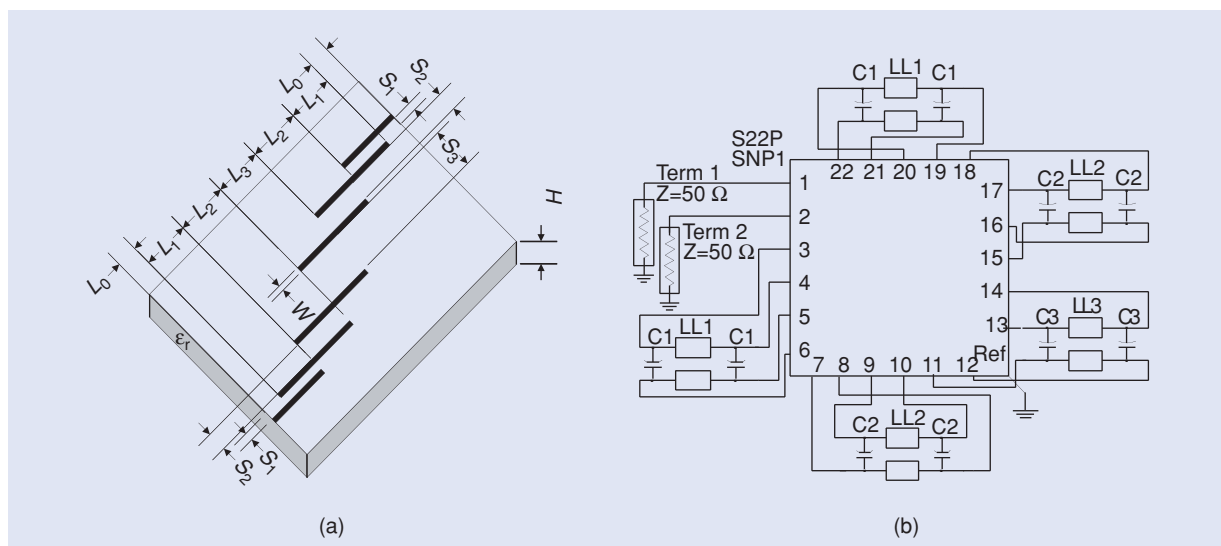


Figure 19. HTS filter: (a) the physical structure [56] and (b) the tuning model (Agilent ADS) [52].

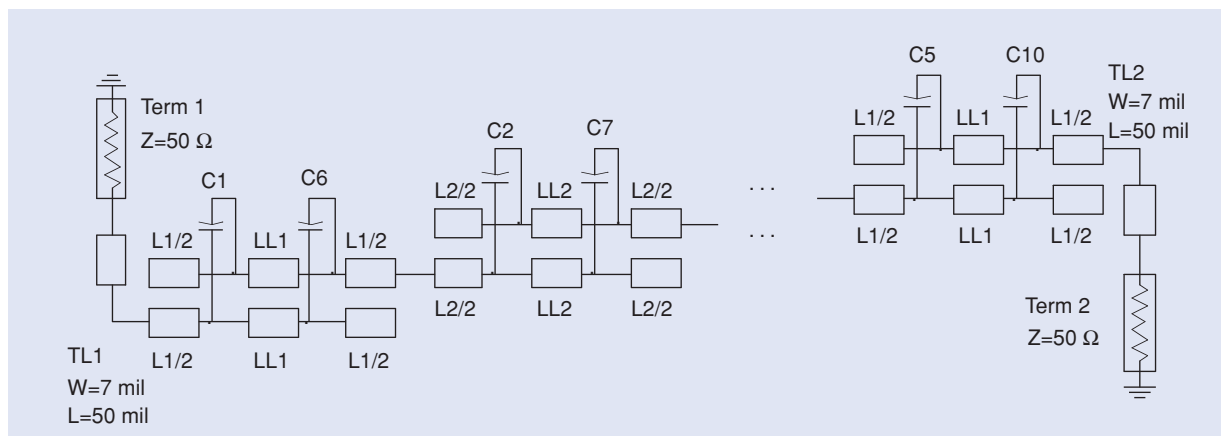


Figure 20. HTS filter: the calibration model (Agilent ADS) [52].

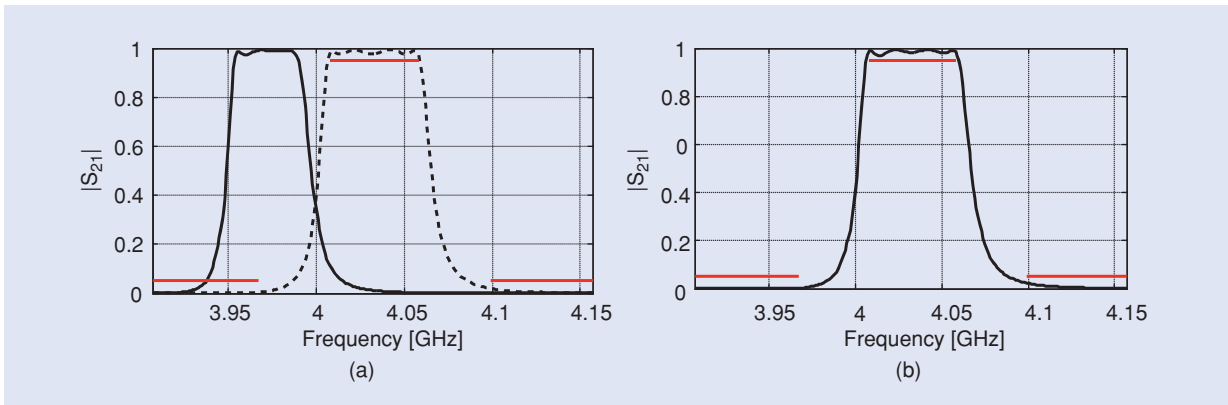


Figure 21. HTS filter: (a) the fine model response at the initial design (solid line) and the response of the optimized tuning model (dashed line) and (b) the fine model response at the final design [52].

a yield estimation at the optimal design with respect to the following specifications: $|S_{21}| \leq 0.05$ for $9.4 \text{ GHz} \leq \omega \leq 10.6 \text{ GHz}$, and $|S_{21}| \geq 0.9$ for $\omega \leq 8 \text{ GHz}$ and $\omega \geq 12 \text{ GHz}$, which is $W_1 = 5.6, W_2 = 10.4, L_0 = 119.2, L_1 = 118.0, L_2 = 112.0$ (dimensions in mil)

assuming tolerances of 0.4 mil for the widths and 2 mil for the lengths. In other words, we want to estimate the percentage of the designs that satisfy the specifications assuming that the geometrical dimensions of the actual fabricated device will deviate from the optimal design up to the given tolerances.

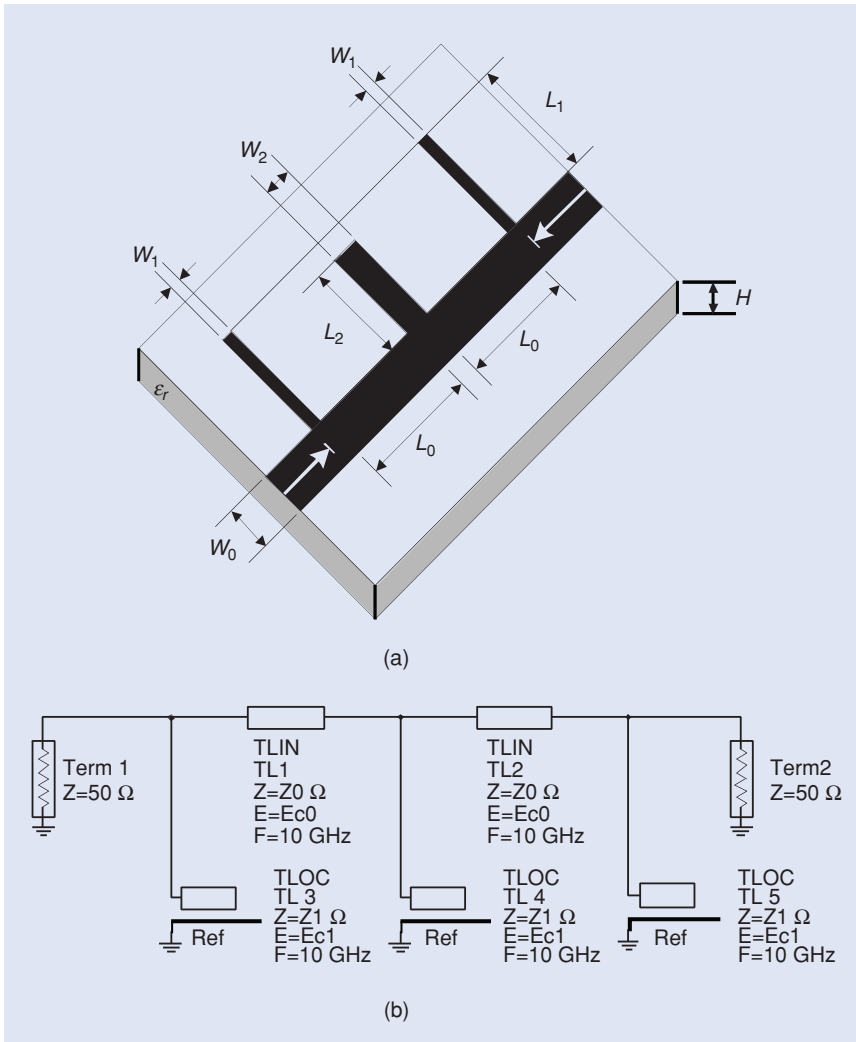


Figure 22. Bandstop microstrip filter: (a) the geometry [63] and (b) the coarse model (Agilent ADS).

Here we can see the results of the yield estimation done with 200 random samples. The plots in Figure 23(a)–(c) show the family of model responses for the fine, coarse, and space-mapping surrogate models. If the estimation is performed using the fine model, we get a value of 63%. If we do the same using just a coarse model we get 0%, which shows that the coarse model is not accurate enough to be used in the analysis in place of the fine model. On the other hand, the yield estimated using the space-mapping surrogate model is 69%, which is pretty good taking into account that only 11 fine model evaluations were used to create the model. In other words, the space mapping surrogate allows us to perform statistical analysis almost 20 times faster than the analysis performed directly with the fine model, and the accuracy is quite decent.

We should mention that space mapping has been successfully combined with functional approximation techniques such as radial basis functions [64] and fuzzy

systems [65], which allows improvement of modeling accuracy when a larger amount of fine model data is available. In such cases, the standard space-mapping model acts as a trend function while the functional layer is used to model the residuals between the fine model and the standard space mapping surrogate at all base points.

Space-Mapping Software

The necessary components for a space-mapping implementation are: a coarse model simulator, a fine model simulator, and a suitable optimization engine. To achieve automatic space-mapping iterations, additional elements, such as sequential calls to the optimization engine and communication between a space-mapping algorithm and the fine model, are necessary. OSA90 [10] demonstrated the first implementation of the original space mapping algorithm [24]. Equipped with a circuit (coarse) simulator, an optimization engine, Empipe [11] and/or Empipe3D [12] (communicating with external fine models) and Datapipe (for sequential calls between optimization engines), OSA90 facilitated the looping of the steps of space mapping.

It is desirable to implement space mapping within commercial EDA software, e.g., Agilent ADS [25]. Bandler et al. [66] introduced a space-mapping design framework that is easy for microwave engineers to follow. Within ADS, the framework implemented input, implicit, and output space mapping.

Space mapping is powerful; however, it is not always straightforward to implement, especially if one wants to use some advanced techniques and employ commercial simulators in the automatic optimization loop. In order to make space mapping accessible to engineers not experienced in this technology, the comprehensive space mapping system SMF was introduced in 2007 by Koziel and Bandler [67]. SMF is a user-friendly, Matlab-based software system that exploits space-mapping technology. SMF can perform space-mapping-based constrained optimization, modeling, and statistical analysis. It implements existing space-mapping approaches, including input, output, implicit, and frequency space mapping [in particular, the generalized implicit space-mapping (GISM) framework [39]]. It contains drivers for simulators (Sonnet *em*, MEFiSTo, Agilent ADS, FEKO, HFSS) that allow the linking of commercial fine/coarse models to the algorithm and make the optimization process fully automatic.

For the sake of brevity, we only discuss the optimization module of the SMF system shown in Figure 24. It contains a number of setup interfaces where the user enters problem arguments, including starting point, and design specifications. The user also sets

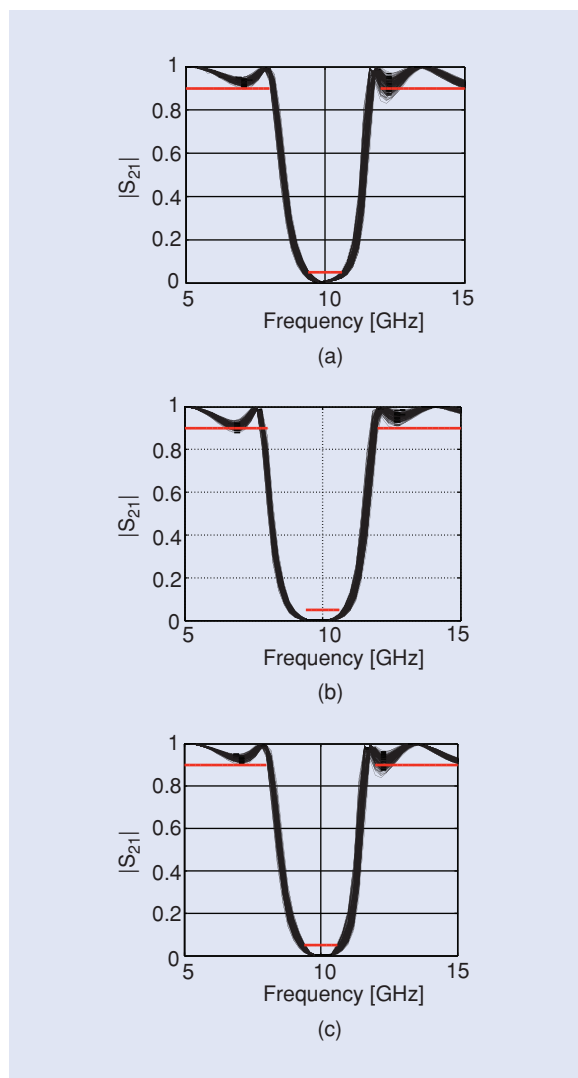


Figure 23. Bandstop microstrip filter: the yield estimation based on 200 random samples for (a) the fine model (63%), (b) the coarse model (0%), and (c) the space mapping surrogate model (69%).

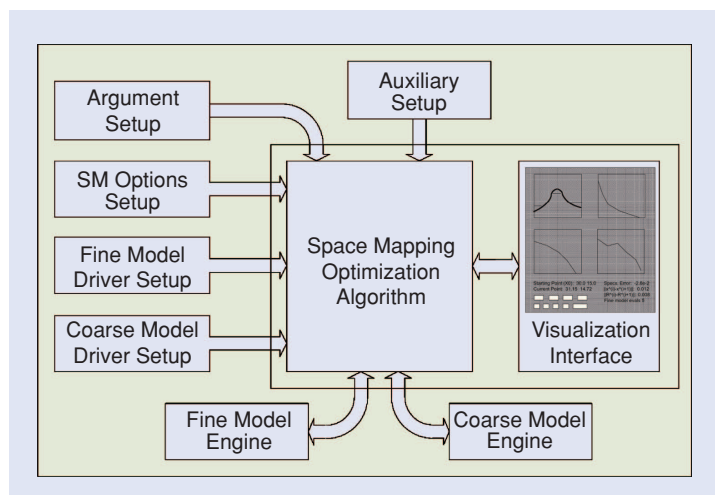


Figure 24. Architecture of the optimization module in the SMF system [67].

up the type of space mapping to be used, specifies termination conditions, parameter extraction options, and optional constraints. The next step is to link the fine and coarse models to SMF by setting up the data (e.g., simulator input files and design variable identification data) that will be used to create model drivers. The drivers are later used to evaluate fine/coarse models for any required design variable values. Having done the setup, the user starts the execution interface, which allows us to run the space-mapping optimization algorithm and visualize the results, including model responses, specification error plots, and convergence plots.

Figure 25 shows the flowchart of the space-mapping optimization process. First, the user needs to set up whatever is necessary as described before including the design specifications and space-mapping type one wants to use as well as the termination condition for the algorithm. The next step is to link fine/coarse models to the system by providing necessary data about the simulator, design variables, and initial design. The initial step of space mapping optimization is typically the optimization of the coarse model. This can be done using a dedicated interface and the coarse model optimal solution can be then used as a starting point for the space-mapping optimization. The actual space-mapping optimization is performed in the execution interface, which contains the response plot, specification error plot, convergence plots, a panel with corresponding numeric values, as well as a number of controls to

run, stop, reset the algorithm, and review it iteration by iteration. The optimization process is fully automatic; however, the user can intervene if necessary.

Discussion

Distinction [68] should be made between space-mapping optimization and optimization based on functional approximations using polynomials [60], radial basis functions [60], kriging [61], etc. The latter methods establish a localized approximation of fine model responses using fine model simulations. Such approximations are typically updated using new fine model points. On the other hand, for a small investment in fine model simulations, space mapping exploits an underlying coarse model (knowledge) that is physically based and capable of accurately simulating the system under consideration over a wide range of parameter values. The surrogate is updated iteratively.

Knowledge-based neural network models [69] and so-called neural space mapping [63] also take advantage of a coarse model to expand the region of validity beyond the range of the training data and/or to reduce the number of data points required in the training process.

Advantages of space mapping can be summarized as follows. It provides an efficient (typically only a few iterations are required) optimization method for expensive models (e.g., EM-simulation-based models). Typically, it does not require fine model derivatives. Space-mapping-based interpolation makes a continuous model

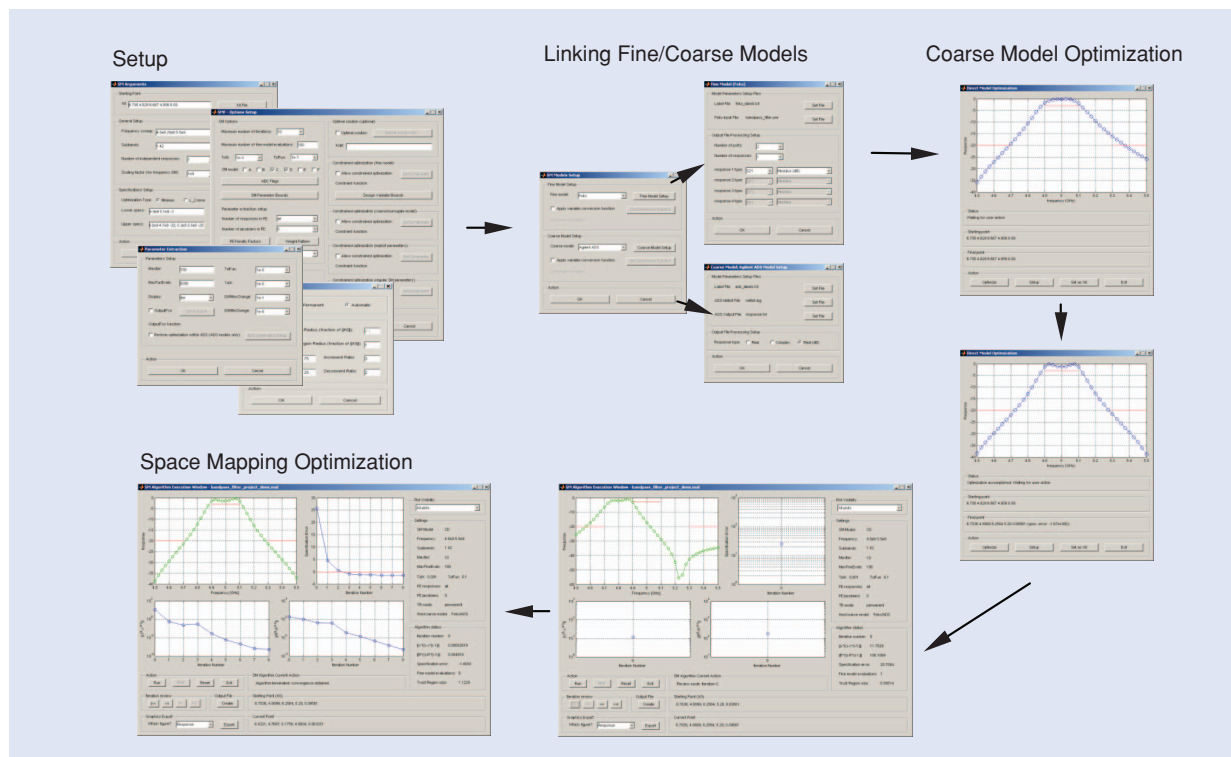


Figure 25. Flowchart of the space-mapping optimization in the SMF system. The process includes setup, linking of the fine/coarse models to the system, coarse model optimization, and automatic space-mapping optimization.

available on a discrete subset of the design space [70]. Fast surrogate optimization allows a larger number of design parameters to be considered [31], [71], which implies a better chance of obtaining a good design. A good surrogate model remains useful after the design process is completed.

Summary

Microwave CAD has its roots in the 1960s [1]. Its practice saw the enrichment of circuit-based model libraries, advances in EM and circuit simulation accuracy, and the refinement of microwave optimization technology. In 1994 [24], space mapping emerged: a powerful yet simple mathematically based technology that takes advantage of progress in the aforementioned key areas. Space mapping has since developed into an approach of choice for EM-based design. In this article, we provided a general framework for the space-mapping optimization concept. We illustrated space-mapping optimization through a simple bandstop filter. We demonstrated the robustness of the technique by performing an accurate design of an interdigital filter. We reviewed state-of-the-art developments in space mapping that feature implicit space mapping, output space mapping, gradient-based space mapping as well as trust region methods; surrogate model choice and adaptive space mapping; tuning space mapping; and space mapping for device modeling. We reviewed implementation techniques and demonstrated the SMF space-mapping software package.

Acknowledgments

This work was supported in part by the Natural Sciences and Engineering Research Council of Canada under Grants RGPIN7239-06, and STPGP336760-06, and by Bandler Corporation.

We thank Sonnet Software, Inc., Syracuse, New York, for *em*, and Agilent Technologies, Santa Rosa, California, for ADS. Jim Rautio of Sonnet Software is thanked for help on novel uses of his software.

We would like to acknowledge various technical collaborators who helped shape our research, including Jie Meng, Mohamed H. Bakr, and Natalia K. Nikolova of McMaster University, Canada; José Rayas-Sánchez of ITESO, Guadalajara, Mexico; Qi-Jun Zhang, Carleton University, Canada; and K. Madsen, Technical University of Denmark, Lyngby, Denmark.

References

- [1] G.C. Temes and D.A. Calahan, "Computer-aided network optimization the state-of-the-art," *Proc. IEEE*, vol. 55, no. 11, pp. 1832–1863, Nov. 1967.
- [2] J.W. Bandler, "Optimization methods for computer-aided design," *IEEE Trans. Microwave Theory Tech.*, vol. MTT-17, no. 8, pp. 533–552, Aug. 1969.
- [3] J.W. Bandler, "Computer-aided circuit optimization," in *Modern Filter Theory and Design*, G.C. Temes and S. K. Mitra, Eds. New York: Wiley, pp. 211–271, 1973.

- [4] G.E. Brehm, "Multifunction MMIC history from a process technology perspective," *IEEE Trans. Microwave Theory Tech.*, vol. 38, no. 9, pp. 1164–1170, Sept. 1990.
- [5] J.W. Bandler, S.H. Chen, S. Daijavad, W. Kellermann, M. Renault, and Q.J. Zhang, "Large scale minimax optimization of microwave multiplexers," in *Proc. European Microwave Conf.*, Dublin, Ireland, Sept. 1986, pp. 435–440.
- [6] J.W. Bandler and S.H. Chen, "Circuit optimization: the state of the art," *IEEE Trans. Microwave Theory Tech.*, vol. 36, no. 2, pp. 424–443, Feb. 1988.
- [7] J.W. Bandler and A.E. Salama, "Functional approach to microwave postproduction tuning," *IEEE Trans. Microwave Theory Tech.*, vol. MTT-33, no. 4, pp. 302–310, Apr. 1985.
- [8] P-N Designs, Inc., "History of microwave software." [Online]. Available: <http://www.microwaves101.com/encyclopedia/historyCAD.cfm>
- [9] J.W. Bandler, P.C. Liu, and H. Tromp, "A nonlinear programming approach to optimal design centering, tolerancing and tuning," *IEEE Trans. Circuits Syst.*, vol. CAS-23, no. 3, pp. 155–165, Mar. 1976.
- [10] OSA90/hope™, version 4.0, User's Manual, August 1997, Optimization Systems Associates Inc. (now Agilent Technologies), Dundas, Ontario, Canada.
- [11] Empipe™, version 4.0, User's Manual, July 1997, Optimization Systems Associates Inc. (now Agilent Technologies), Dundas, Ontario, Canada.
- [12] Empipe3D™, version 4.0, User's Manual, June 1997, Optimization Systems Associates Inc. (now Agilent Technologies), Dundas, Ontario, Canada.
- [13] J.W. Bandler, R.M. Biernacki, S.H. Chen, P.A. Grobelny, and S. Ye, "Yield-driven electromagnetic optimization via multilevel multi-dimensional models," *IEEE Trans. Microwave Theory Tech.*, vol. 41, no. 12, pp. 2269–2278, Dec. 1993.
- [14] J.W. Bandler, R.M. Biernacki, and S.H. Chen, "Parameterization of arbitrary geometrical structures for automated electromagnetic optimization," *Int. J. RF Microwave CAE*, vol. 9, no. 2, pp. 73–85, Feb. 1999.
- [15] J.W. Bandler, R.M. Biernacki, S.H. Chen, D.G. Swanson, Jr., and S. Ye, "Microstrip filter design using direct EM field simulation," *IEEE Trans. Microwave Theory Tech.*, vol. 42, no. 7, pp. 1353–1359, July 1994.
- [16] J.W. Bandler, R.M. Biernacki, S.H. Chen, W.J. Getsinger, P.A. Grobelny, C. Moskowitz, and S.H. Talisa, "Electromagnetic design of high-temperature superconducting microwave filters," *Int. J. Microwave Millimeter-Wave CAE*, vol. 5, no. 5, pp. 331–343, Sept. 1995.
- [17] J.W. Bandler, R.M. Biernacki, S.H. Chen, L.W. Hendrick, and D. Omeragic, "Electromagnetic optimization of 3-D structures," *IEEE Trans. Microwave Theory Tech.*, vol. 45, no. 5, pp. 770–779, May 1997.
- [18] D.G. Swanson, Jr., "Optimizing a microstrip bandpass filter using electromagnetics," *Int. J. Microwave Millimeter-Wave CAE*, vol. 5, no. 5, pp. 344–351, Sep. 1995.
- [19] D.G. Swanson, Jr., "Computer aided design of passive components," in *The RF and Microwave Handbook*, M. Golio, Ed. Boca Raton, FL: CRC Press, 2000, pp. 8-34–8-44.
- [20] D.G. Swanson, Jr. and W.J.R. Hoefler, *Microwave Circuit Modeling Using Electromagnetic Field Simulation*. Norwood, MA: Artech House, 2003.
- [21] <http://www.bandler.com/mileston2.htm>
- [22] A. Dounavis, E. Gad, R. Achar, and M.S. Nakhla, "Passive model reduction of multiport distributed interconnects," *IEEE Trans. Microwave Theory Tech.*, vol. 48, no. 12, pp. 2325–2334, Dec. 2000.
- [23] A.H. Zaabab, Q.J. Zhang, and M.S. Nakhla, "A neural network modeling approach to circuit optimization and statistical design," *IEEE Trans. Microwave Theory Tech.*, vol. 43, no. 6, pp. 1349–1358, June 1995.
- [24] J.W. Bandler, R.M. Biernacki, S.H. Chen, P.A. Grobelny, and R.H. Hemmers, "Space mapping technique for electromagnetic optimization," *IEEE Trans. Microwave Theory Tech.*, vol. 42, no. 12, pp. 2536–2544, Dec. 1994.
- [25] Agilent ADS 2005A, Agilent Technologies, Santa Rosa, CA USA.
- [26] Agilent Momentum 2005A, Agilent Technologies, Santa Rosa, CA USA.
- [27] Sonnet *em* Version 11.52, Sonnet Software, Inc., North Syracuse, NY USA.

- [28] Ansoft HFSS Version 10.1, Ansoft Corporation, Pittsburgh, PA USA.
- [29] FEKO User's Manual, Suite 4.2, June 2004, EM Software & Systems-S.A. (Pty) Ltd., Stellenbosch, South Africa. Available: <http://www.feko.info>.
- [30] MEFiSTo-3D Pro, Version 3.0, Faustus Scientific Corp., Victoria, BC, Canada.
- [31] Q.S. Cheng, J.W. Bandler, and S. Koziel, "Combining coarse and fine models for optimal design," *IEEE Microwave Mag.*, vol. 9, no. 1, pp. 79–88, Feb. 2008.
- [32] A.J. Booker, J.E. Dennis, Jr., P.D. Frank, D.B. Serafini, V. Torczon, and M.W. Trosset, "A rigorous framework for optimization of expensive functions by surrogates," *Structural Optimization*, vol. 17, no. 1, pp. 1–13, Feb. 1999.
- [33] A.M. Pavio, "The electromagnetic optimization of microwave circuits using companion models," presented at Workshop on Novel Methods for Device Modeling and Circuit CAD, IEEE MTT-S Int. Microwave Symp., Anaheim, CA, 1999.
- [34] D. Swanson and G. Macchiarella, "Microwave filter design by synthesis and optimization," *IEEE Microwave Mag.*, vol. 8, no. 2, pp. 55–69, Apr. 2007.
- [35] D. Swanson, Jr., "Narrow-band microwave filter design," *IEEE Microwave Mag.*, vol. 8, no. 5, pp. 105–114, Oct. 2007.
- [36] R.J. Cameron and M. Yu, "Design of manifold coupled multiplexers," *IEEE Microwave Mag.*, vol. 8, no. 5, pp. 46–59, Oct. 2007.
- [37] J.W. Bandler, A.S. Mohamed, and M.H. Bakr, "TLM-based modeling and design exploiting space mapping," *IEEE Trans. Microwave Theory Tech.*, vol. 53, no. 9, pp. 2801–2811, Sept. 2005.
- [38] J.C. Rautio, "EM-component-based design of planar circuits," *IEEE Microwave Mag.*, vol. 8, no. 4, pp. 79–90, Aug. 2007.
- [39] S. Koziel, J.W. Bandler, and K. Madsen, "A space mapping framework for engineering optimization: theory and implementation," *IEEE Trans. Microwave Theory Tech.*, vol. 54, no. 10, pp. 3721–3730, Oct. 2006.
- [40] Matlab, Version 7.1, The MathWorks, Inc., Natick, MA, 2005.
- [41] J.W. Bandler, R.M. Biernacki, S.H. Chen, and Y.F. Huang, "Design optimization of interdigital filters using aggressive space mapping and decomposition," *IEEE Trans. Microwave Theory Tech.*, vol. 45, no. 5, pp. 761–769, May 1997.
- [42] J.W. Bandler, Q.S. Cheng, N.K. Nikolova, and M.A. Ismail, "Implicit space mapping optimization exploiting preassigned parameters," *IEEE Trans. Microwave Theory Tech.*, vol. 52, no. 1, pp. 378–385, Jan. 2004.
- [43] Q.S. Cheng and J.W. Bandler, "An implicit space mapping technique for component modeling," in *Proc. 36th European Microwave Conf.*, Manchester, UK, Sept. 2006, pp. 458–461.
- [44] A. Manchec, C. Quendo, J.-F. Favennec, E. Rius, and C. Person, "Synthesis of capacitive-coupled dual-behavior resonator (CCDBR) filters," *IEEE Trans. Microwave Theory Tech.*, vol. 54, no. 6, pp. 2346–2355, June 2006.
- [45] J.W. Bandler, Q.S. Cheng, D.H. Gebre-Mariam, K. Madsen, F. Pedersen, and J. Søndergaard, "EM-based surrogate modeling and design exploiting implicit, frequency and output space mappings," in *IEEE MTT-S Int. Microwave Symp. Dig.*, Philadelphia, PA, June 2003, pp. 1003–1006.
- [46] N.M. Alexandrov and R.M. Lewis, "An overview of first-order model management for engineering optimization," *Optimization Eng.*, vol. 2, no. 4, pp. 413–430, Dec. 2001.
- [47] A. Hennings, E. Semouchkina, A. Baker, and G. Semouchkin, "Design optimization and implementation of bandpass filters with normally fed microstrip resonators loaded by high-permittivity dielectric," *IEEE Trans. Microwave Theory and Tech.*, vol. 54, no. 3, pp. 1253–1261, Mar. 2006.
- [48] A.R. Conn, N.I.M. Gould, and P.L. Toint, *Trust Region Methods*, MPS-SIAM Series on Optimization. Philadelphia, PA: Society for Industrial and Applied Mathematics, 2000.
- [49] S. Koziel and J.W. Bandler, "Space-mapping optimization with adaptive surrogate model," *IEEE Trans. Microwave Theory Tech.*, vol. 55, no. 3, pp. 541–547, Mar. 2007.
- [50] S. Koziel and J.W. Bandler, "Coarse and surrogate model assessment for engineering design optimization with space mapping," *IEEE MTT-S Int. Microwave Symp. Dig.*, Honolulu, HI, June 2007, pp. 107–110.
- [51] S. Koziel, J.W. Bandler, and K. Madsen, "Quality assessment of coarse models and surrogates for space mapping optimization," *Optimization Eng.*, vol. 9, no. 4, pp. 375–391, Dec. 2008.
- [52] J. Meng, S. Koziel, J.W. Bandler, M.H. Bakr, and Q.S. Cheng, "Tuning space mapping: A novel technique for engineering design optimization," in *IEEE MTT-S Int. Microwave Symp. Dig.*, Atlanta, GA, June 2008, pp. 991–994.
- [53] J.C. Rautio, "RF design closure—companion modeling and tuning methods," *IEEE MTT-S IMS Workshop: Microwave component design using space mapping technology*, San Francisco, CA, 2006.
- [54] D.G. Swanson and R.J. Wenzel, "Fast analysis and optimization of combline filters using FEM," in *IEEE MTT-S Int. Microwave Symp. Dig.*, Boston, MA, July 2001, pp. 1159–1162.
- [55] J.W. Bandler, R.M. Biernacki, S.H. Chen, R.H. Hemmers, and K. Madsen, "Electromagnetic optimization exploiting aggressive space mapping," *IEEE Trans. Microwave Theory Tech.*, vol. 43, no. 12, pp. 2874–2882, Dec. 1995.
- [56] J.W. Bandler, R.M. Biernacki, S.H. Chen, W.J. Getsinger, P.A. Grobelyny, C. Moskowitz, and S.H. Talisa, "Electromagnetic design of high-temperature superconducting microwave filters," *Int. J. RF Microwave CAE*, vol. 5, no. 5, pp. 331–343, Sept. 1995.
- [57] S. Koziel, J.W. Bandler, A.S. Mohamed, and K. Madsen, "Enhanced surrogate models for statistical design exploiting space mapping technology," in *IEEE MTT-S Int. Microwave Symp. Dig.*, Long Beach, CA, June 2005, pp. 1609–1612.
- [58] S. Koziel, J.W. Bandler, and K. Madsen, "Theoretical justification of space-mapping-based modeling utilizing a data base and on-demand parameter extraction," *IEEE Trans. Microwave Theory Tech.*, vol. 54, no. 12, pp. 4316–4322, Dec. 2006.
- [59] J.E. Rayas-Sánchez and V. Gutiérrez-Ayala, "EM-based Monte Carlo analysis and yield prediction of microwave circuits using linear-input neural-output space mapping," *IEEE Trans. Microwave Theory Tech.*, vol. 54, pp. 4528–4537, Dec. 2006.
- [60] T.W. Simpson, J.D. Peplinski, P.N. Koch, and J.K. Allen, "Metamodels for computer-based engineering design: Survey and recommendations," *Eng. Comput.*, vol. 17, no. 2, pp. 129–150, July 2001.
- [61] T.W. Simpson, T.M. Maurey, J.J. Korte, and F. Mistree, "Kriging models for global approximation in simulation-based multidisciplinary design optimization," *AIAA J.*, vol. 39, no. 12, pp. 2233–2241, Dec. 2001.
- [62] J.E. Rayas-Sánchez, "EM-based optimization of microwave circuits using artificial neural networks: the state of the art," *IEEE Trans. Microwave Theory Tech.*, vol. 52, no. 1, pp. 420–435, Jan. 2004.
- [63] M.H. Bakr, J.W. Bandler, M.A. Ismail, J.E. Rayas-Sánchez, and Q.J. Zhang, "Neural space mapping optimization for EM-based design," *IEEE Trans. Microwave Theory Tech.*, vol. 48, no. 12, pp. 2307–2315, Dec. 2000.
- [64] S. Koziel and J.W. Bandler, "Microwave device modeling using space-mapping and radial basis functions," in *IEEE MTT-S Int. Microwave Symp. Dig.*, Honolulu, HI, June 2007, pp. 799–802.
- [65] S. Koziel and J.W. Bandler, "A space-mapping approach to microwave device modeling exploiting fuzzy systems," *IEEE Trans. Microwave Theory and Tech.*, vol. 55, no. 12, pp. 2539–2547, Dec. 2007.
- [66] J.W. Bandler, Q.S. Cheng, D.M. Hailu, and N.K. Nikolova, "A space-mapping framework," *IEEE Trans. Microwave Theory Tech.*, vol. 52, no. 11, pp. 2601–2610, Nov. 2004.
- [67] S. Koziel and J.W. Bandler, "SMF: A user-friendly software engine for space-mapping-based engineering design optimization," in *Proc. Int. Symp. Signals, Systems and Electronics*, URSI ISSSE 2007, Montreal, Canada, July 2007, pp. 157–160.
- [68] M.H. Bakr, J.W. Bandler, K. Madsen, and J. Søndergaard, "Review of the space mapping approach to engineering optimization and modeling," *Optimization Eng.*, vol. 1, no. 3, pp. 241–276, Sept. 2000.
- [69] F. Wang and Q.J. Zhang, "Knowledge based neural models for microwave design," *IEEE Trans. Microwave Theory Tech.*, vol. 45, no. 12, pp. 2333–2343, Dec. 1997.
- [70] S. Koziel, J.W. Bandler, and K. Madsen, "Space-mapping based interpolation for engineering optimization," *IEEE Trans. Microwave Theory and Tech.*, vol. 54, no. 6, pp. 2410–2421, June 2006.
- [71] Q.S. Cheng, J.W. Bandler, and J.E. Rayas-Sánchez, "Tuning-aided implicit space mapping," *Int. J. RF Microwave CAE*, vol. 18, no. 5, pp. 445–453, Sept. 2008.

